Eur Biophys J (2010) 39:1625–1635
DOI 10.1007/s00249-010-0620-0

ORIGINAL PAPER

Biophysical characterization of the fluorescent protein voltage probe VSFP2.3 based on the voltage-sensing domain of Ci-VSP

Alicia Lundby · Walther Akemann · Thomas Knöpfel

Received: 9 March 2010 / Revised: 13 July 2010 / Accepted: 19 July 2010 / Published online: 6 August 2010

Abstract A voltage sensitive phosphatase was discovered in the ascidian *Ciona intestinalis*. The phosphatase, Ci-VSP, contains a voltage-sensing domain homologous to those known from voltage-gated ion channels, but unlike ion channels, the voltage-sensing domain of Ci-VSP can reside in the cell membrane as a monomer. We fused the voltage-sensing domain of Ci-VSP to a pair of fluorescent reporter proteins to generate a genetically encodable voltage-sensing fluorescent probe, VSFP2.3. VSFP2.3 is a fluorescent voltage probe that reports changes in membrane potential as a FRET (fluorescence resonance energy transfer) signal. Here we report sensing current measurements from VSFP2.3, and show that VSFP2.3 carries 1.2 e sensing charges, which are displaced within 1.5 ms. The sensing currents become faster at higher temperatures, and the voltage dependence of the decay time constants is temperature dependent. Neutralization of an arginine in S4, previously suggested to be a sensing charge, and measuring associated sensing currents indicate that this charge is likely to reside at the membrane-aqueous interface rather than within the membrane electric field. The data presented give us insights into the voltage-sensing mechanism of Ci-VSP, which will allow us to further improve the sensitivity and kinetics of the family of VSFP proteins.

Keywords Ci-VSP · VSFP · Voltage sensing fluorescent proteins · Fluorescent voltage probe

A. Lundby · W. Akemann · T. Knöpfel
Laboratory for Neuronal Circuit Dynamics, RIKEN Brain Science Institute, Wako-City, Saitama 351-0198, Japan

A. Lundby
The Danish National Research Foundation Centre for Cardiac Arrhythmia, The Panum Institute, University of Copenhagen, Copenhagen, Denmark

A. Lundby (✉)
The Novo Nordisk Foundation Center for Protein Research, The Panum Institute, University of Copenhagen, Copenhagen, Denmark
e-mail: alicia.lundby@cpr.ku.dk

Introduction

Voltage sensors of voltage-gated ion channels operate the opening and closing of a membrane pore. The voltage-sensing domains (VSDs) have distinct conformational states, and their equilibrium positions are directly dependent on the membrane potential. As the transition between conformational states governs a translocation of charged amino acids in the VSD, it can be measured in the external circuit as a transient current, which is known as gating current (Bezanilla 2000). VSDs homologous to those of voltage-gated potassium channels (Kv channels) have recently been identified in voltage-sensor-domain-protein families (Okamura 2007). These proteins include Ci-VSP (*Ciona intestinalis* voltage-sensing phosphatase), which is a phosphatase with voltage-dependent activity (Murata et al. 2005), and VSOP (voltage sensor domain only protein), which operates as a proton channel consisting of an isolated VSD (Ramsey et al. 2006; Sasaki et al. 2006). Unlike the tetrameric structure known from ion channels, Ci-VSP reportedly resides in the membrane as a monomer (Kohout et al. 2008), whereas VSOP is a dimer (Koch et al. 2008).

We have recently developed a family of artificial voltage-sensitive fluorescent proteins (VSFPs), where a VSD controls the fluorescence read-out of a pair of fluorescent proteins. The design concept of these genetically encodable voltage probes is that a change in the membrane potential

causes a transition in the conformational state of the VSD, which is transduced to a fluorescent protein reporter, such that the optical output of the probe is modulated by the membrane potential. The latter can for instance be achieved through a modulation of FRET between a pair of CFP and YFP (cyan and yellow fluorescent proteins). That is, in the same way that the membrane potential modifies the open probability of voltage-gated ion channels, it modifies the fluorescence read-out of these VSFPs. Our first generation of VSFPs was based on a Kv channel VSD (VSFP1) (Sakai et al. 2001; Knöpfel et al. 2003). Exchanging the VSD with the one from Ci-VSP greatly improved targeting of the sensor to the plasma membrane in mammalian cells and led to the second generation VSFP (VSFP2) (Dimitrov et al. 2007). Even though our design strategy led to successful generation of a functional VSFP, it was unclear whether the observed function was actually determined by the envisioned mechanism. For further development of VSFPs, it is important to understand the operational transitions of the protein to identify which components are the limiting factors for such features as speed of sensing and signal-to-noise ratio of the fluorescence output. With this aim we started to analyze sensing current measurements from the voltage probe variant VSFP2.3. We use the term 'sensing current' instead of the 'gating currents' described in ion channels to underscore that there is no gating of a channel pore. We found the voltage-sensing charge displacements of the probe to be remarkably fast with a time constant in the range of 0.5–1 ms at physiologically relevant voltages (Lundby et al. 2008). It was surprising to us that the VSD of Ci-VSP can operate on such a fast timescale, firstly because equivalent measurements performed on *Xenopus* oocytes revealed time constants that are ten times slower (Villalba-Galea et al. 2008a) and secondly because sensing current measurements from Ci-VSP pointed to the voltage-sensing mechanism of this protein to be relatively slow (time constant ~30 ms) (Murata et al. 2005). The apparent discrepancy between time constants measured from *Xenopus* oocytes and mammalian cells might be due to the VSD of Ci-VSP behaving differently in these lipid environments. Indeed, Ci-VSP sensing current measurements from the same laboratory revealed much slower sensing currents in oocytes than in mammalian cells (Murata et al. 2005; Hossain et al. 2008).

Here we extend our investigation of VSFP2.3-sensing currents aiming at a better understanding of the voltage-sensing mechanism of VSFP2.3 and at the same time obtaining information on the voltage sensor of Ci-VSP. We find that VSFP2.3 carries 1.2 *e* sensing charges that are associated with fast sensing currents and that it has comparable potentials for half-maximal activation for 'on'- and 'off'-sensing. From our sensing current measurements, we estimate the average density of VSFP2.3 molecules to approximately 300/μm^2 in stably expressing PC12 cells. Investigation of an arginine to glutamine mutation in S4 known to greatly left-shift the voltage-dependency indicates that this charge is not a sensing charge, unlike what has been suggested in previous studies (Kohout et al. 2008; Sasaki et al. 2006), but rather resides at a position that interacts with parts of the protein that rearrange as the VSD undergoes its conformational change. We further show that VSFP2.3 operation is only slightly temperature dependent, with the greatest effect of temperature being on the activation/decay time constants.

Materials and methods

Molecular biology

PC12 cells (ATCC) were grown in high-glucose DMEM (Gibco-Invitrogen) supplemented with 5% fetal calf serum and 10% horse serum on poly-D-lysine-coated coverslips. The R217Q mutation was introduced in VSFP2.3 by site-directed mutagenesis and verified by DNA sequencing. Recordings were either performed on wild-type PC12 cells (control), a PC12 cell-line stably expressing VSFP2.3 or PC12 cells transiently transfected with VSFP2.3 (Q217R). Transfections were done 1 day after plating using Lipofectamine 2000 (Invitrogen) reagent according to the manufacturer's instructions. Recordings from transiently expressing PC12 cells were performed 48–72 h post-transfection.

Electrophysiology and fluorescence measurements

All experimental procedures for electrophysiology and fluorescence recordings were done as previously described (Lundby et al. 2008) with the temperature in the recording chamber being varied between 25, 30 and 35°C by an in-line temperature controller. A coverslip with PC12 cells was placed in a recording chamber mounted on the stage of an inverted microscope (Eclipse TE-2000, Nikon), and voltage-clamp recordings in the whole-cell configuration were performed using an Axopatch 200B amplifier (Axon Instruments). Recording solutions contained in mM: 140 NMDG, 10 HEPES, 1 $MgCl_2$, 1.8 $CaCl_2$, 10 dextrose and pH 7.2 using HCl for the pipette; and 140 NMDG, 10 HEPES, 5 EGTA, 1 $MgCl_2$ and pH 7.4 using HCl for the bath, where NMDG is N-methyl-D-glucamine. Two to four fluorescence traces were elicited from a holding potential of −70 mV by a sequence of 20-mV activation steps lasting 500 ms to a final potential of 110 mV with 10 s interpulse intervals and averaged for each cell. Three to seven sensing current traces were recorded from each cell

by 20 ms potential steps in the range from −90 to +110 mV in 20 mV steps with a 5 s interpulse interval from a holding potential of −70 mV and averaged. Data were acquired at 50 kHz and filtered by a 5 kHz low-pass Bessel filter.

Fluorescence was induced by light (440 nm) from a computer controlled monochromator (Polychrome IV, T.I.L.L. Photonics) through a 50× oil immersion objective. Fluorescence emission was collected through the objective and directed via a first dichroic mirror (DCLP 445 nm) through a beam splitter (DCLP505) and an emission filter (D480/40) onto two photodiodes (Viewfinder, T.I.L.L. Photonics). Photodiode signals were digitized along with the electrophysiological signals using Axon hard- and software as described above. For the experiments photobleaching YFP, the images were obtained with a Nikon confocal laser scanning microscope (C1si/FN1, Nikon, Japan) using a 40× water immersion objective in "true color" display mode. A 440 nm wavelength diode laser was used to excite fluorescence, and the fluorescence emission spectrum was collected by an array of 64 photomultipliers. YFP was photo-bleached by excitation at 488 nm using an argon laser.

Data analysis

Sensing currents and fluorescence signals were analyzed as previously described (Lundby et al. 2008) using Clampfit 9.2 (Axon Instruments), OriginPro 7 (OriginLab) and Excel (Microsoft) software. Photobleaching was manually corrected, fluorescence transients elicited by voltage steps were fit with single exponential functions, and the amplitude of fluorescence transients was measured at the end of a test pulse and expressed as percentage of baseline fluorescence. Sensing currents were extracted from recorded current traces by subtraction of linear leak current and linear capacitive transients. Leak current was subtracted by measuring the mean current amplitude in the last 2 ms of the hyperpolarizing voltage step and subtracting a correspondingly scaled Ohmic current from each recorded current trace. Similarly, the capacitive transient needed to charge the cell membrane was estimated by a single-exponential fit to the current recorded at the hyperpolarizing voltage step, and a linear voltage-dependent exponential was subtracted from each current trace recorded. The sensing current charge displacement was estimated as the time integral of the 'on'-sensing current. Steady-state current-voltage relations recorded from single cells were normalized and fitted with a two-state Boltzmann function, $I/I_{max} = (1 + \exp((-z_g F(V–V_{½}))/(RT)))^{-1}$, where z_g is the sensing charge valence, F is the Faraday constant, R is the gas constant, and T is the absolute temperature. Values for half maximal activation, $V_{½}$, and slope factors, a, were calculated as mean values obtained from the ensemble of cells. The apparent sensing charge was estimated from the slope factor using the formula $a = RT/(z_g F)$. The dependence of the time constant for a given transition on the absolute temperature is given by the Arrhenius equation $\ln(1/\tau) = -E_a/RT + \ln(1/\tau_0)$ where E_a is the activation energy, R is the gas constant, T is the absolute temperature, and τ_0 is a constant of the reaction. When the Arrhenius plot gives a straight line, the activation energy of the process is a constant and can be found from the slope. The temperature coefficient Q_{10} for transition between two states was calculated from $\tau_1/\tau_2 = Q_{10}\text{^}(T_2 - T_1)/10$. All data points are represented by mean values, and error bars indicate standard error of the mean.

Results

Measuring VSFP2.3 sensing currents

VSFP2.3 was designed by fusing the VSD from Ci-VSP to a pair of CFP/YFP chromophores (Fig. 1a). The protein targets to the plasma membrane of PC12 cells (Fig. 1b), and donor dequenching experiments confirm that there is FRET between the CFP and YFP (Fig. 1c). We previously demonstrated for this series of fusion proteins that membrane depolarization increases the YFP spectral component and decreases the CFP spectral component, indicating that the FRET is modulated by membrane voltage (Mutoh et al. 2009; Dimitrov et al. 2007, cf, Fig. 3a). We would like to note, however, that the voltage response of VSFP2.3 and similar constructs also involves a FRET-independent component (for details, see Lundby et al. 2008; Perron et al. 2009). As gating charge movement provides a direct measure of the voltage sensor operation, we set out to investigate the VSD movements of VSFP2.3 by measuring sensing currents from a PC12 cell line stably expressing the protein. Cells were patch-clamped in the whole cell configuration using extra- and intracellular solutions based on the membrane impermeable cation N-methyl-D-glucamine (NMDG+) in order to isolate the sensing currents (Wang et al. 2007). Unless stated otherwise, sensing currents were recorded from a holding potential of −70 mV, and a test pulse to −90 mV was used to estimate the amplitude of currents arising from the membrane capacitance and the leak current. Non-transfected PC12 cells did not reveal non-linear voltage-dependent capacitive currents. That is, the amplitude of endogenous gating currents in undifferentiated PC12 cells was below the resolution of our measurements. We therefore concluded that the sensing currents measured in VSFP2.3 expressing PC12 cells were not contaminated by endogenous gating currents (Fig. 2a). In contrast, the PC12 cell line stably expressing VSFP2.3

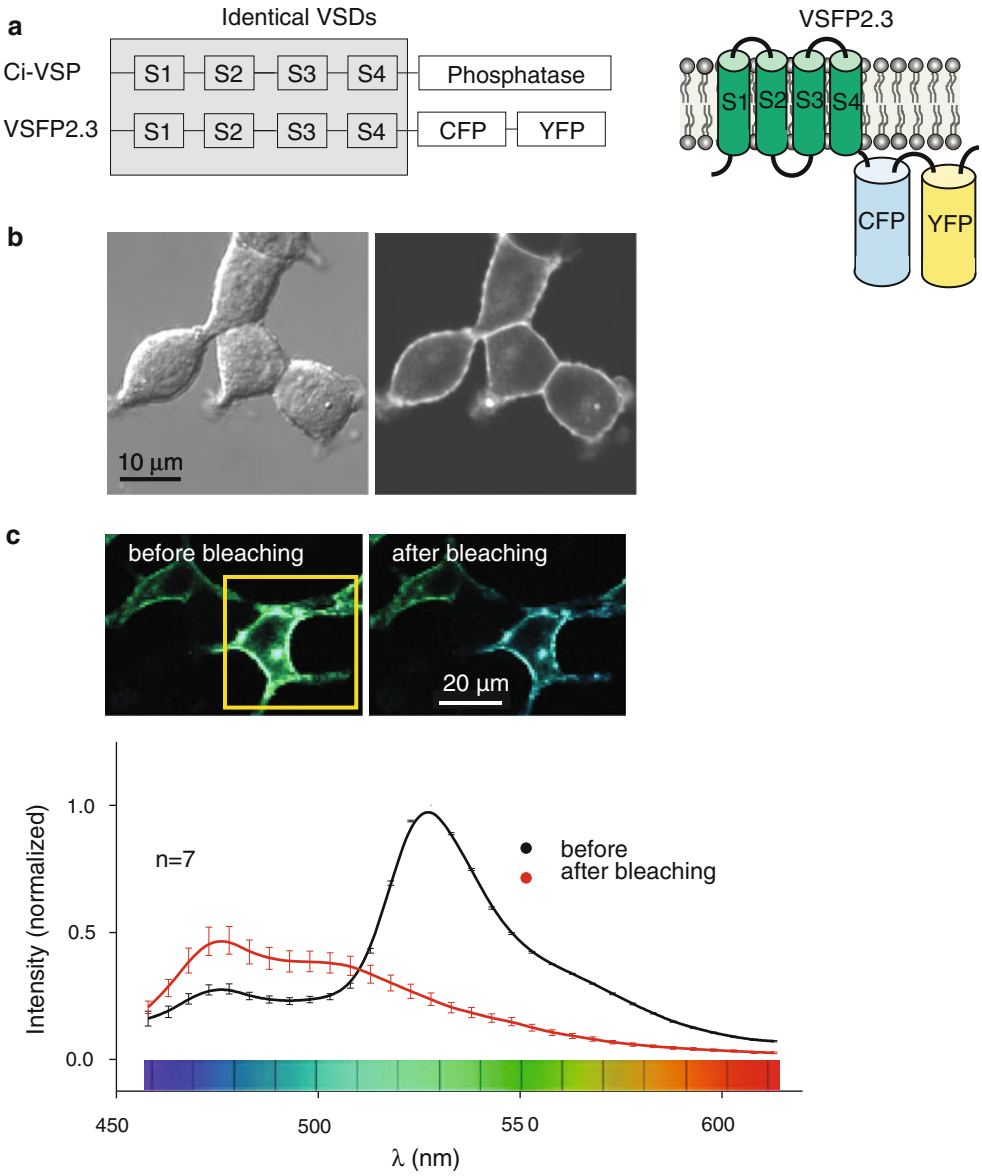

Fig. 1 VSFP2.3 design features. **a** The voltage-sensing domain of VSFP2.3 is similar to the one for Ci-VSP except for a R217Q mutation in S4. Instead of the phosphatase present in Ci-VSP, the VSFP2.3 construct contains a pair of CFP and YFP fluorescent proteins. Topologically, the voltage-sensing domain of VSFP2.3 resides in the plasma membrane, whereas the fluorescent reporter proteins reside in the cytosol. **b** Transmission and fluorescence images of PC12 cells stably expressing VSFP2.3. Note the membrane expression of the protein. **c** True-color fluorescence images of PC12 cells expressing VSFP2.3 before and after photobleaching of YFP. Photobleaching of YFP (*yellow rectangle*) abolishes the spectral component corresponding to YFP and increases the spectral component corresponding to CFP

consistently produced voltage-dependent current transients amounting to a couple of hundred picoamperes in amplitude (Fig. 2b).

Conformational transitions in VSFP2.3

At the same time that we recorded sensing currents, we measured VSFP2.3 fluorescence read-outs. Representative fluorescence responses elicited from VSFP2.3 by voltage steps are shown in Fig. 3a. The amplitude of the fluorescence read-out was measured at the end of the test pulse and expressed as percentage of baseline fluorescence. As previously shown, 'on'-sensing currents and the fluorescence read-out have comparable, although statistically different, potentials for half-maximal activation (-17.4 ± 1.5 mV vs. -23.9 ± 2.1 mV), indicating that the 'on'-activation of the VSD in the steady state is reliably reported in the optical readout (Lundby et al. 2008). This relationship is further supported by the observation that for each cell the quantity of sensing charge transferred upon activation correlates with the amplitude of the fluorescence response (Fig. 3b). That is, the greater the amplitude of 'on'-sensing currents from a particular cell is, the greater is the measured change in fluorescence read-out.

Sensing current measurements provide information on the transmembrane movement of charge associated with transitions between different conformational states. In Fig. 3c, we show the voltage dependence of the charge displacement in the 'on'- as well as in the 'off'-sensing reactions in order to compare the transitions taking place. As is evident from the figure, the two activation curves are very similar except for a small difference in the potential

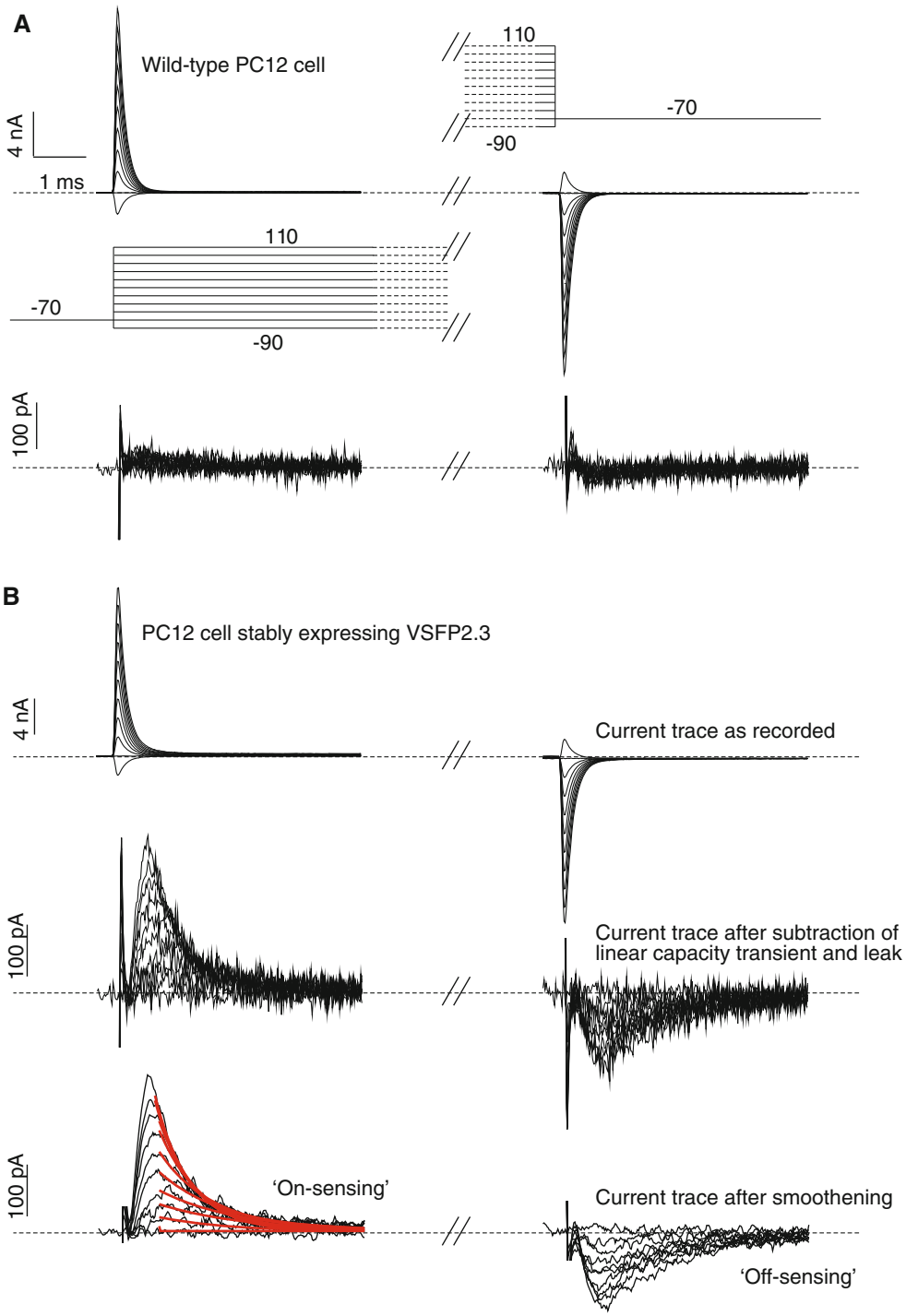

Fig. 2 Measuring sensing currents from PC12 cells. **a** Control recordings from wild-type PC12 cells elicit capacitance transients and leak currents upon multiples of 20 mV voltage steps between −90 and 110 mV lasting 20 ms each with a 5 s interpulse interval from a holding potential of −70 mV (*top panel*). Subtraction of voltage-independent capacitance transient and leak current as estimated from the pulse to −90 mV show that PC12 cells have negligible levels of endogenous gating currents (*lower panel*). The spike in the beginning of the pulse is an artifact from the subtraction procedure and is blocked in later figures. **b** Similar recordings performed on a PC12 cell line stably expressing VSFP2.3. Current traces before (*top panel*) and after (*middle panel*) subtraction of the voltage-independent capacitance currents needed to charge the cell membrane as well as the leak current are shown. The lower panel shows the current traces after smoothing the curves by 5-point averaging for 'on'- and 'off'-sensing currents. The 'on'-sensing decays are superimposed by single exponential fits

of their half-maximal activation (−17.4 ± 1.5 mV vs −22.3 ± 2.6 mV), which might be due to differences in charge transferred. The charge transferred in the 'on'- and the 'off-reaction' at a test potential of 70 mV is shown for ten different cells in Fig. 3d. Linear regression through the data points gives $R^2 = 0.88$, and the small inset shows that the ratio of charge transferred in the 'on'- and 'off'-reactions is close to one at all potentials tested. Similar measurements carried out for Ci-VSP likewise show almost equal charge movement for 'on'- and 'off'-sensing (Hossain et al. 2008).

From the measurement of the sensing charges, we estimated the density of VSFP2.3 molecules in the cell membrane. For ten cells the measured average sensing charge for a voltage step from −70 to 0 mV was 134.5 ± 16.1 fC, and the average membrane capacitance

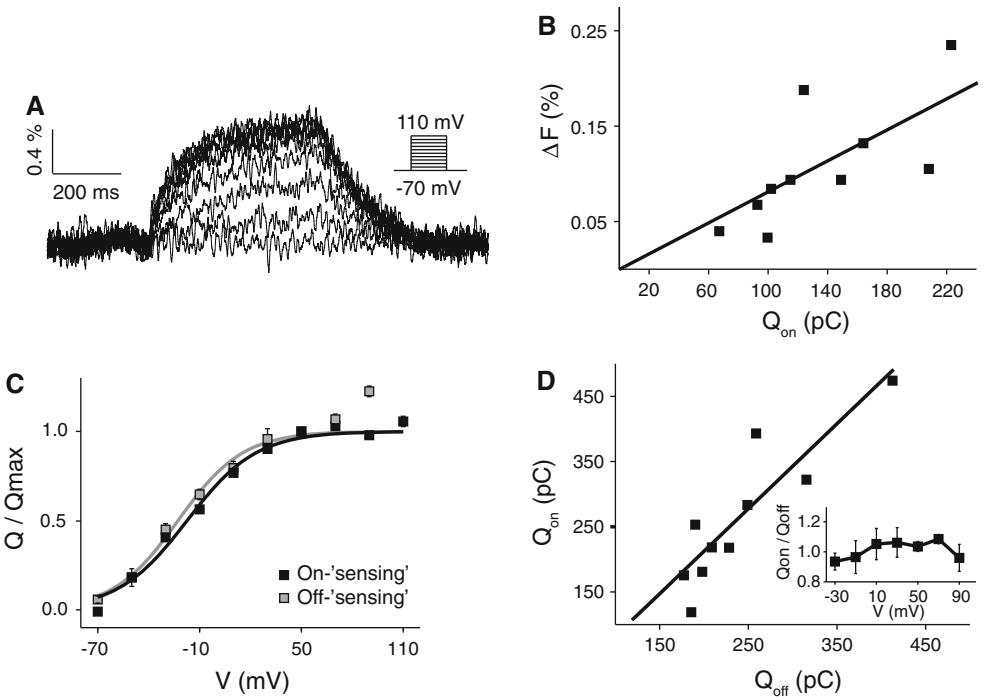

Fig. 3 Characterization of VSFP2.3 voltage responses. **a** Representative fluorescence responses measured in the yellow channel elicited from a single PC12 cell stably expressing VSFP2.3 upon a voltage step protocol as indicated. *Scale bar* indicates $\Delta F/F$. **b** Relation between the measured charge transfer for 'on'-sensing and the change in yellow fluorescence observed upon a voltage step to 70 mV for ten different cells. Linear regression through the data points gives $R^2 = 0.5$. **c** Voltage dependence of charge transfer for 'on'-sensing as well as for 'off'-sensing. **d** Correlation between the charge transferred in 'on'-sensing and in 'off'-sensing measured at 70 mV for ten cells. The *inset* shows the ratio of charge transferred in 'on'-sensing and 'off'-sensing as a function of test potential for three cells

was 24.7 ± 1.60 pF, thus resulting in a mobile charge of 5.45 nC per microfarad of membrane capacity. Estimating the specific capacitance of the cell membrane as 1 μF/cm^2 gives a charge movement of 5.45 nC/cm^2, or 3.40 × 10^{10} *e*/cm^2 in elementary charges. From the steepness of the voltage dependence of sensing a lower limit for the magnitude of the sensing charge per VSFP2.3 molecule can be calculated (Hille 1992). Thus, as the fit of a two-state Boltzmann function to the 'on'-sensing measurements reveals a slope factor of $a = 20.4 \pm 0.9$ mV, we calculate that VSFP2.3 carries an apparent sensing charge of 1.25 *e*, under the simplifying assumption that the voltage dependence of VSFP2.3 can be described as a two-state process (see "Methods"). Using this **lower** limit of the magnitude of sensing charges per molecule, the **maximal** average density of VSFP2.3 molecules is 272 VSFP2.3 molecules per μm^2 in the stably expressing PC12 cell line. This value falls within the wide range of densities reported for native ion channel protein in excitable membranes. While, for instance, the density of Na^+ channels can be as low as 2–10 channels per μm^2 of somatic and dendritic membranes of neurons (Magee and Johnston 1995), it can reach ~1,500 channels per μm^2 of membrane in the axon node (Hille 1992). For further development of fluorescent protein voltage sensors, it will be important to investigate what density of the sensor is acceptable in a cell membrane before interference with physiologic processes become apparent.

Is position 217 a sensing charge residue?

Introduction of a Q217R mutation in VSFP2.3 greatly right-shifts the activation curve of its fluorescence output (Dimitrov et al. 2007). Likewise, we here find that the mutation causes a shift of the sensing currents by 107 mV (from −17.4 ± 1.5 mV to 90.0 ± 1.5 mV, Fig. 4b). Evaluation of the Boltzmann fits for the two constructs reveals slope factors of $a = 20.4 \pm 0.9$ mV and $a = 23.8 \pm 0.9$ mV, respectively. Following the same calculation as before, we estimate 1.07 *e* as the lower limit of the sensing charge of VSFP2.3(Q217R) as compared to 1.25 *e* for VSFP2.3. Figure 4c shows the voltage dependence of the 'on'-sensing decay time constants for the two proteins. The measurements for VSFP2.3 are taken from Lundby et al. 2008 and are indicated in grey. It is clearly seen that the voltage-sensing mechanism of the VSFP protein is slowed by the Q217R mutation, as the 'on'-sensing decay time range for VSFP2.3 is 0.5–1.4 ms versus 1.1–2.6 ms for VSFP2.3(Q217R). Introduction of a positively charged arginine at position 217 thus causes a right-shift of the

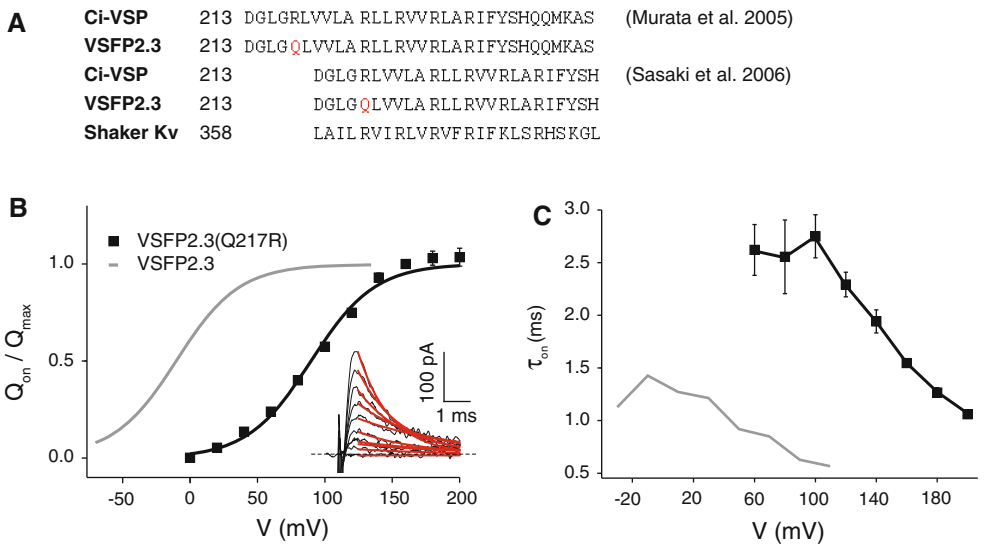

Fig. 4 Effect of Q217R mutation on VSFP2.3 sensing currents. **a** Amino acid sequence alignments of VSP2.3, Ci-VSP and *Shaker* Kv channel. Two alignments for VSFP2.3 and *Shaker* are shown based on differing alignments proposed for Ci-VSP (*top*). Alignments consistent with the data presented in this paper are shown below. **b** The *Q-V* curve for VSFP2.3(Q217R) 'on'-sensing was obtained by normalizing time integrals of current traces as shown in the inset. For comparison, the Boltzmann fit to the corresponding data for VSFP2.3 is shown in *grey*. Representative 'on'-sensing currents recorded from VSFP2.3(Q217R) are shown as an *inset* superimposed with single exponential fits of the decay of the currents. The time constants derived from similar fits as function of the clamp potential for VSFP2.3(Q217R) are shown in (**c**). For comparison, the corresponding data recorded from VSFP2.3 are shown in grey (data in *grey* taken from Lundby et al. 2008)

activation curve, leads to a reduction of sensing charge, and slows down the operation of the VSD. Taken together, these findings suggest that a charged amino acid at position 217 is not a sensing charge. Several sequence alignments for the VSD of Ci-VSP have been suggested in the literature (see Fig. 4). Our finding of residue 217 not being a sensing charge correlates with the alignment presented by Alabi et al. (2007). This alignment is further in accordance with the finding that the charged residues at positions 229 and 232 of Ci-VSP are required to detect sensing currents (Murata et al. 2005), and these positions hence define the intracellular end of the transmembrane portion of S4. Under the assumption that the VSFP2.3 VSD folds similarly to the one of Ci-VSP, this would locate position 217 of VSFP2.3 in close proximity to the membrane-aqueous interface.

Temperature dependence of VSFP2.3 gating currents

To gain additional insights into the activation reaction of VSFP2.3, we investigated the temperature dependence of VSFP2.3 activation kinetics by recording fluorescence responses and sensing currents at three different temperatures. It should be noted that the fluorescence signals were fitted with a single time constant and hence represent mainly the dominant slower kinetic component of the VSFP2.3 response (Mutoh et al. 2009). Figure 5a shows the voltage dependence of the fluorescence response from VSFP2.3 measured at 25, 30 and 35°C, respectively. Increasing the temperature caused only a modest right-shift of the fluorescence activation curve, but it had a pronounced effect on the apparent activation time constant, reducing it from ~100 to ~50 ms at the most depolarized potentials (Fig. 5b, Table 1). The apparent fluorescence activation time is only slightly dependent on voltage. To evaluate the effect of temperature on the activation of the VSD, the decaying phase of the 'on'-sensing currents were fitted with single exponential functions, and the time constants were plotted as a function of the clamp potential (Fig. 5c, d). The activation time constants exhibit voltage as well as temperature dependency. At the smaller depolarizations, the reaction is about twice as fast at 35°C as at 25°C. At depolarizations greater than +70 mV, the measured activation time was identical at all temperatures tested. It thus appears that the process of activation at its fastest is undertaken in ~0.5 ms under the present experimental conditions. However, this value might reflect technical limitations to voltage clamping the cell and extracting sensing currents rather than reflecting limitations in the VSFP2.3 sensing kinetics. Figure 5e, f shows Arrhenius plots for the activation ($1/\tau_{on}$) and deactivation ($1/\tau_{off}$) rate constants against temperature. The corresponding activation energies are found to be close to 7 kcal/mol at −30 and 70 mV for the activation reaction, and the temperature coefficient is calculated to be 1.4 at both potentials. For the deactivation reaction measured at

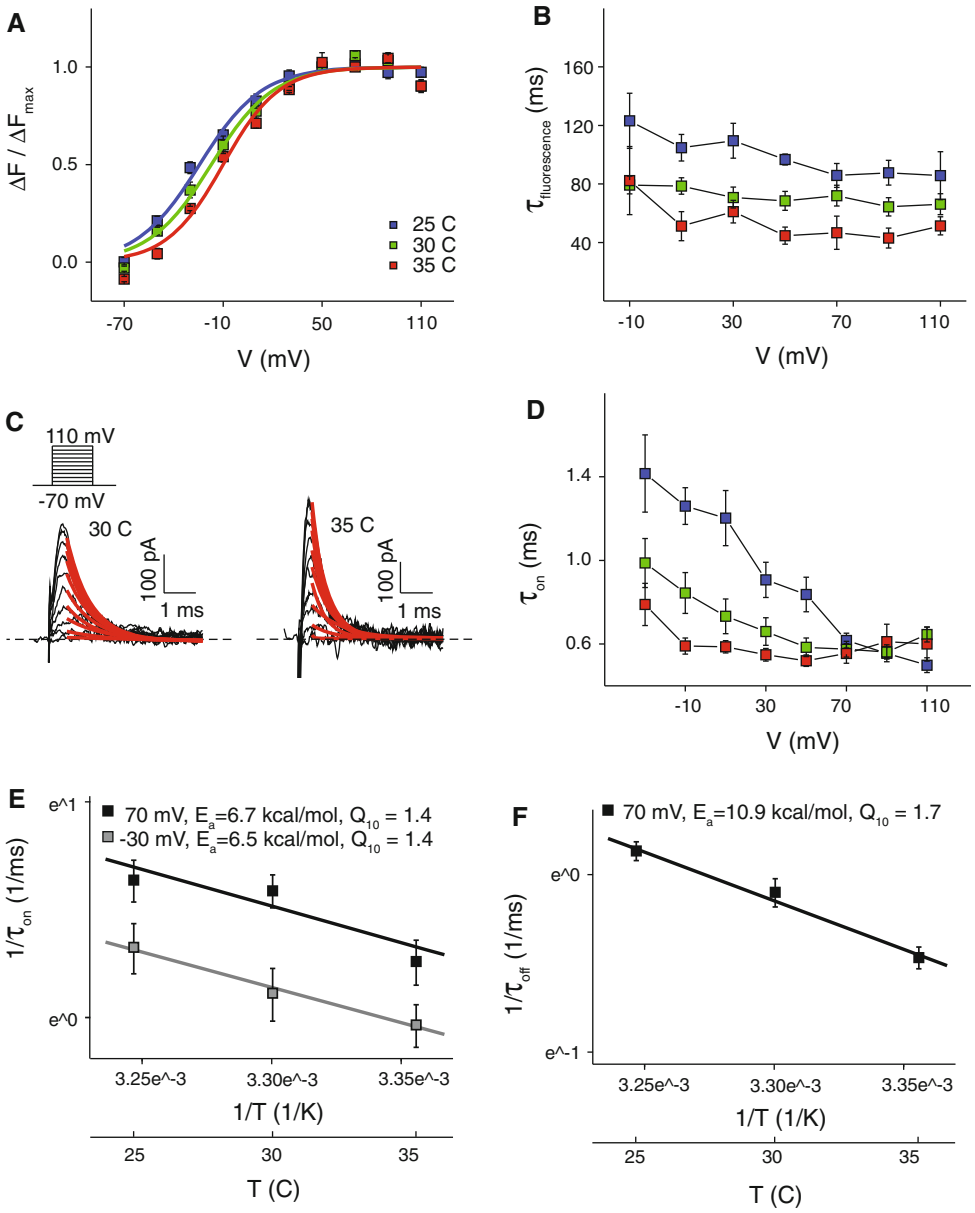

Fig. 5 Temperature dependence of VSFP2.3 sensing currents. **a** Voltage dependence of yellow fluorescence response for VSFP2.3 measured at 25, 30 and 35°C. **b** Activation time constants for the fluorescence response from VSFP2.3 measured at the same three temperatures. **c** Representative 'on'-sensing currents for VSFP2.3 superimposed with single exponential fits for the decay measured at 30 and 35°C. **d** Voltage dependency of time constants of 'on'-sensing decay measured at three temperatures as indicated. **e** Semi-log Arrhenius plot of the temperature dependence of rate constants for 'on'-sensing decay measured at −30 and 70 mV. Activation energies estimated from the linear regression slopes and calculated Q_{10} values are indicated. **f** Semi-log Arrhenius plot of rate constants for 'off'-sensing rising phase as a function of temperature recorded at −70 mV after a prepulse at +70 mV

Table 1 Parameters measured from VSFP2.3 sensing currents and fluorescence response at three temperatures

Temp (°C)		Fluorescence			Sensing current		
		25	30	35	25	30	35
ΔF	$V_{1/2}$ (mV)	−23.9 ± 2.1	−17.2 ± 3.2	−9.8 ± 1.5			
	a (mV)	19.3 ± 1.2	18.0 ± 0.4	17.1 ± 1.03			
Q_{on}	$V_{1/2}$ (mV)				−17.4 ± 1.5	−24.5 ± 2.9	−24.2 ± 2.5
	a (mV)				20.4 ± 0.9	18.9 ± 0.9	20.5 ± 1.3
Q_{off}	$V_{1/2}$ (mV)				−22.3 ± 2.6	−30.7 ± 4.9	−29.6 ± 2.8
	a (mV)				19.3 ± 1.2	17.8 ± 1.3	15.8 ± 3.0
τ_{on} at 0 mV (ms)		85.8 ± 8.1	72.0 ± 7.1	46.7 ± 11.3	0.84 ± 0.08	0.58 ± 0.04	0.55 ± 0.05
τ_{off} at 0 mV (ms)		137.0 ± 22.0	70.6 ± 9.7	49.3 ± 5.2	1.65 ± 0.11	1.16 ± 0.10	1.16 ± 0.05

70 mV, the activation energy is found to be 10.9 kcal/mol, and the calculated Q_{10} value is 1.7. These results suggest that there is only a modest temperature dependence of the VSFP2.3 activation kinetics and that the main temperature effects are on the time constants for the fluorescence response as well as for the sensing current. The finding that the voltage dependency of the decay time constant for the 'on'-sensing differs with temperature suggests that the VSD transitions captured in the sensing currents have different temperature dependency. These observations are in agreement with recent voltage clamp fluorometry measurements that indicate multiple components of the voltage-dependent rearrangements of Ci-VSP (Kohout et al. 2008; Villalba-Galea et al. 2008a, b).

Discussion

Transitions captured by sensing currents and fluorescence signals

We investigated the voltage-sensing mechanism of VSFP2.3, and hence indirectly that of the VSD of Ci-VSP, by measuring sensing currents from a PC12 cell line stably expressing the protein. We found the voltage dependence of the fluorescence response to closely mimic that of sensing currents (Lundby et al. 2008) and the amplitude of the fluorescence response to be proportional to the amount of sensing current. These observations suggest that the conformational transitions captured by the sensing currents trigger the fluorescence signal. However, the difference in the kinetics of the sensing current (time scale $\sim$1 ms) and of the fluorescence response with a dominant process of slower kinetics (time scale $\sim$80 ms) indicates a reaction pathway of the fluorescence response that involves an additional kinetic reaction step subsequent to the transfer of sensing charge. This interpretation is consistent with the higher activation energy of the optical signal compared to that of the sensing currents as evident from our temperature-dependence measurements. It should be noted that sensing currents only capture movement of charges in the direction of the membrane electric field, whereas the fluorescence signal can report additional conformational transitions either directly reflecting movement of charged residues or conformational transitions that are triggered by the former. In this sense, the fluorescence signal of VSFP2.3 contains information similar to that obtained by voltage-clamp fluorometry (Claydon et al. 2007; Pathak et al. 2007; Villalba-Galea 2008a, b).

For Ci-VSP it has been shown that the activated position of its VSD is not stable, thus causing the VSD to relax into a lower energy conformational state at prolonged depolarizations (Villalba-Galea et al. 2008b). Using pulse protocols with prolonged depolarizations, Villalba-Galea and colleagues provided evidence that the same holds true for VSFP2.3. After prolonged depolarization of the membrane, the voltage-sensing domain of VSFP2.3 relaxes into a new conformational state, which causes the activation curve to shift in the negative direction (Villalba-Galea et al. 2008a). Comparing fluorescence and electrophysiological data from VSFP2.3 with those of fluorescently labeled Ci-VSP suggests that the conformational changes of VSFP2.3 that are reflected by the slow kinetic component of the VSFP2.3 voltage response correspond to the depolarization-induced relaxation of the VSD (Villalba-Galea et al. 2009). These observations provide a plausible explanation for the apparent discrepancy between the fast kinetics of the VSFP2.3 sensing charge motion and the measured fluorescence response, which is dominated by a kinetic component that is considerably slower (see also Lundby et al. 2008). In addition to the dominating slow component, the VSFP2.3 fluorescence response also exhibits a fast component of smaller amplitude that activates in close synchrony with the charge movement as most clearly seen in recordings from VSFP2.3 in oocytes (Villalba-Galea et al. 2009). This fast component of the fluorescence response, though also present in VSFP2.3 responses recorded in PC12 cells at physiological temperature (Mutoh et al. 2009), remains ambiguous in the present fluorescence measurements as these were obtained at room temperature and with experimental conditions optimized for simultaneous record of VSFP2.3 sensing currents.

Residues contributing to sensing currents

Sensing currents represent movement of VSD charges forced by a change in the transmembrane electric field. Assuming that the VSD carrying these sensing charges can be modeled as a simple rigid body, and its movement by a two-state Boltzmann function, leads to the expectation that neutralizing a positively charged residue at a sensing position (e.g., that contributes to the sensing charges) would decrease the sensing charge (i.e., decrease the steepness of the Boltzmann curve), slow down the sensing mechanism and right-shift the activation curve. However, voltage sensing mechanisms appear more complex than this, and neutralization of a presumed sensing charge can also cause a left-shift of the activation curve (Papazian et al. 1991; Liman et al. 1991). Although the activation curve can be either left- or right-shifted by neutralization of a residue that provides the sensing charge, we would associate a specific residue with sensing charges only if neuralization of its charge reduces the total sensing charge and slows the sensing mechanism. In this study we investigated sensing currents from VSFP2.3 and

VSFP2.3(Q217R), where VSFP2.3(Q217R) has a VSD identical to the one of Ci-VSP and VSFP2.3 has a VSD corresponding to Ci-VSP(R217Q). Our measurements demonstrate that the protein containing the positively charged arginine at position 217 (as in the wild-type Ci-VSP) exhibit a reduced apparent sensing charge (1.07*e* vs. 1.25*e*) and a slower sensing mechanism (the time constant of the decay of the 'on'-sensing current is more than two-fold greater) in addition to a dramatically right-shifted activation curve (Dimitrov et al. 2007; Kohout et al. 2008) compared to the protein containing a neutral glutamine at that position. The observed decrease in sensing charge and the slowing of the sensing mechanism in presence of an arginine at position 217 are not in line with the above predicted properties of a sensing charge. We therefore conclude that R217 in Ci-VSP is not a sensing charge. Additional circumstantial evidence for Ci-VSP residue 217 to be outside the sensing region of S4 is the observation that a V220R mutation in VSFP2.3 causes a 50-mV right-shift in the fluorescence response curve (Mutoh and Knöpfel, unpublished observation).

Similar to our findings, in the mVSOP channel, the R201Q mutation (corresponding to R217Q in Ci-VSP) leads to a left-shift of the activation curve of 50 mV and an increase in valence charge of 0.5 *e* (Sasaki et al. 2006), thus suggesting that the mVSOP residue homologous to Ci-VSP 217 is not a sensing position. However, a similar mutation in the human proton channel Hv1 leads to a 40-mV left-shift of the activation curve, but decreases the valence charge by 0.3 *e* (Ramsey et al. 2006).

Our evidence against position 217 being a sensing charge sheds new light on the homology alignments of the S4 segments of Ci-VSP and Kv channels that are presented in the literature. In one proposed alignment, arginine 217 is homologous to a sensing charge in the *Shaker* Kv channel (Kohout et al. 2008; Sasaki et al. 2006), whereas in another alignment residue 217 is outside the sensing region of S4 (Fig. 4a) (Alabi et al. 2007; Murata et al. 2005). Our data support the latter alignment. As Ci-VSP residues 229 and 232 are required for detecting sensing currents from Ci-VSP (Murata et al. 2005), this suggests that position 217 of Ci-VSP (and VSFP2.3) is located near the outer membrane-aqueous interface.

Based on the functional analogies of VSFP2.3 and mVSOP and the results discussed above, we propose residue 217 of Ci-VSP to be aligned as suggested in Fig. 4a. Then why does mutation of residue 217 affect the voltage dependence of VSFP2.3/Ci-VSP? One possible explanation for this is that the arginine at position 217 interacts with parts of the VSD that undergo a conformational change during sensing and opposes the movement of the VSD by providing an additional energy barrier for the voltage sensor to overcome upon activation.

Multiple states

Measuring reaction rates at several temperatures gives insights as to the transitions taking place in a particular reaction. This is due to the dependence of reaction rates on activation energies, which have entropic as well as enthalpic components. The enthalpic and entropic components will change differently with temperature, and thus allow for distinguishing between different energetic components to the reaction rate (Rodriguez et al. 1998). We characterized the energetics of VSFP2.3 activation using temperature studies and found the Q_{10} values to be in the range of 1.4–1.7 for the potentials tested. Hence, the kinetics of the VSFP2.3 voltage response do not exhibit strong temperature dependence, but it does become slightly faster at higher temperatures. As the voltage dependence of single components can differ with temperature due to the individual transitions having different enthalpic and entropic components (Rodriguez et al. 1998), our finding that the voltage dependency of the 'on'-sensing time constant changed with temperature suggests that the voltage-sensing mechanism is likely a multiple-state process. This conclusion is consistent with our earlier observation that a multiple-state reaction pathway is required to account for the measured kinetic properties of VSFP2.3 (Akemann et al. 2009).

Future directions

Investigating sensing currents from the fluorescent protein voltage sensor VSFP2.3 gives us insights into the molecular transitions the protein undergoes upon activation. Such understanding is important for further development of this class of biosensors, including tuning of the sensor to the desired application system. Once a sufficient molecular understanding is attained, it would be advantageous to use a combined approach of experimentally testing modified VSFP proteins and applying computer simulations to explore a wider parameter space (Akemann et al. 2009) to address which are the essential parameters to improve to obtain a biosensor with properties fine-tuned to the cellular network of interest.

References

Akemann W, Lundby A, Mutoh H, Knöpfel T (2009) Effect of voltage sensitive fluorescent proteins on neuronal excitability. Biophys J 96:3959–3976

Alabi AA, Bahamonde MI, Jung HJ, Kim JI, Swartz KJ (2007) Portability of paddle motif function and pharmacology in voltage sensors. Nature 450:370–375

Bezanilla F (2000) The voltage sensor in voltage-dependent ion channels. Physiol Rev 80:555–592

Claydon TW, Vaid M, Rezazadeh S, Kwan DCH, Kehl SJ, Fedida D (2007) A direct demonstration of closed-state inactivation of K+ channels at low pH. J Gen Physiol 129:437–455

Dimitrov D, He Y, Mutoh H, Baker BJ, Cohen L, Akemann W, Knöpfel T (2007) Engineering and characterization of an enhanced fluorescent protein voltage sensor. PLoS One 2:e440

Hille B (1992) Ionic channels of excitable membranes. Sinauer Associates, Sunderland

Hossain MI, Iwasaki H, Okochi Y, Chahine M, Higashijima SI, Nagayama K, Okamura Y (2008) Enzyme domain affects the movement of the voltage sensor in ascidian and zebrafish VSPs. J Biol Chem 26:18248–18259

Knöpfel T, Tomita K, Shimazaki R, Sakai R (2003) Optical recordings of membrane potential using genetically targeted voltage-sensitive fluorescent proteins. Methods 30:42–48

Koch HP, Kurokawa T, Okochi Y, Sasaki M, Okamura Y, Larsson HP (2008) Multimeric nature of voltage-gated proton channels. Proc Natl Acad Sci USA 105:9111–9116

Kohout SC, Ulbrich MH, Bell SC, Isacoff EY (2008) Subunit organization and functional transitions in Ci-VSP. Nat Struct Mol Biol 15:106–108

Liman ER, Hess P, Weaver F, Koren G (1991) Voltage-sensing residues in the S4 region of a mammalian K+ channel. Nature 353:752–756

Lundby A, Mutoh H, Dimitrov D, Akemann W, Knöpfel T (2008) Engineering of a genetically encodable fluorescent voltage sensor exploiting fast Ci-VSP voltage-sensing movements. PLoS One 3:e2514

Magee JC, Johnston D (1995) Characterization of single voltage-gated Na+ and Ca2+ channels in apical dendrites of rat CA1 pyramidal neurons. J Physiol 487:67–90

Murata Y, Iwasaki H, Sasaki M, Inaba K, Okamura Y (2005) Phosphoinositide phosphatase activity coupled to an intrinsic voltage sensor. Nature 435:1239–1243

Mutoh H, Perron A, Dimitrov D, Iwamoto Y, Akemann W, Chudakov DM, Knöpfel T (2009) Spectrally-resolved response properties of the three most advanced FRET based fluroescent protein voltage probes. PLoS One 4:e4555

Okamura Y (2007) Biodiversity of voltage sensor domain proteins. Pflugers Arch-European J Physiol 454:361–371

Papazian DM, Timpe LC, Jan YN, Jan LY (1991) Alteration of voltage-dependence of *Shaker* potassium channel by mutations in the S4 sequence. Nature 349:305–310

Pathak MM, Yarov-Yarovoy V, Agarwal G, Roux B, Barth P, Kohout S, Tombola F, Isacoff EY (2007) Closing in on the resting state of the shaker K+ channel. Neuron 56:124–140

Perron A, Mutoh H, Launey T, Knöpfel T (2009) Red-shifted voltage-sensitive fluorescent proteins. Chem Biol 16:1268–1277

Ramsey IS, Moran MM, Chong JHA, Clapham DE (2006) A voltage-gated proton-selective channel lacking the pore domain. Nature 440:1213–1216

Rodriguez BM, Sigg D, Bezanilla F (1998) Voltage gating of shaker K+ channels—the effect of temperature on ionic and gating currents. J Gen Physiol 112:223–242

Sakai R, Repunte-Canonigo V, Raj CD, Knöpfel T (2001) Design and characterization of a DNA-encoded, voltage-sensitive fluorescent protein. Eur J Neurosci 13:2314–2318

Sasaki M, Takagi M, Okamura Y (2006) A voltage sensor-domain protein is a voltage-gated proton channel. Science 312:589–592

Villalba-Galea CA, Dimitrov D, Mutoh H, Lundby A, Sandtner W, Bezanilla F, Knöpfel T (2008a) Charge movement of the Voltage Sensitive Fluorescent Protein. Biophys J 94:1362

Villalba-Galea CA, Sandtner W, Starace DM, Bezanilla F (2008b) S4-based voltage sensors have three major conformations. Proc Natl Acad Sci USA 105:17600–17607

Villalba-Galea CA, Sandtner W, Dimitrov D, Mutoh H, Knöpfel T, Bezanilla F (2009) Charge movement of a voltage-sensitive fluorescent protein. Biophys J 96:19–21

Wang ZR, Robertson B, Fedida D (2007) Gating currents from a Kv3 subfamily potassium channel: charge movement and modification by BDS-II toxin. J Physiol -Lond 584:755–767